ELSEVIER

Journal of Nuclear Materials 281 (2000) 91–105

journal of nuclear materials

www.elsevier.nl/locate/jnucmat

Kinetic and thermodynamic study of the thorium phosphate–diphosphate dissolution

A.C. Thomas [a], N. Dacheux [a,*], P. Le Coustumer [b], V. Brandel [a], M. Genet [a]

[a] *Groupe de Radiochimie, Institut de Physique Nucléaire, Bât. 100, Université de Paris-Sud-XI, 91406 Orsay cedex, France*
[b] *LMGE, UMR-CNRS 6532, ESIP, 40 av. Pineau, 86022 Poitiers, France*

Received 26 June 2000; accepted 24 July 2000

Abstract

The dissolution of the thorium phosphate–diphosphate (TPD), which was proposed for the actinides immobilization, was systematically studied as a function of several parameters such as surface, leaching flow, temperature, acidity or basicity of the leachate and phosphate concentration. The dependence of the normalized leaching rate on the temperature leads to an activation energy equal to about 42 ± 3 kJ mol^{-1}. The normalized leaching rate is slightly increased when increasing the acidity or the basicity of the leachate. The partial orders related to proton and hydroxide ions are equal to 0.31–0.35 and 0.35, respectively. For the pH range studied, i.e., $1 < \text{pH} < 4$ and $10 < \text{pH} < 13$, the normalized dissolution rate is always lower than 10^{-5} g m^{-2} d^{-1} which confirms the good retention properties of the TPD even in a very corrosive medium. The presence of phosphate ions in the solution slightly increases the normalized leaching rate, but this increase is significant only for concentration higher than 0.1 M. Simultaneously to these experiments, the TEM study showed the formation of an amorphous external thin layer on the TPD surface and small corrosion pits during the first days of leaching in 5 M HNO_3. Several crystallized phases coexist inside the gel finally obtained after the rather complete dissolution of TPD. When the saturation of the solution is obtained, the neoformed phase was identified as the thorium phosphate–hydrogen phosphate hydrate whose solubility product is very small. In these conditions, the thorium and phosphate concentrations measured in the leachate are controlled by the precipitation of such a compound and remain lower than 10^{-5} M when the initial TPD is partly dissolved.

1. Introduction

In the framework of the nuclear waste storage, many authors already reported the potential use of phosphate matrices like apatites, monazites or NZP for the immobilization of actinides [1–3]. In this field, the chemistry of thorium phosphates was completely re-examined. We found that several compounds mentioned in the literature such as $Th_3(PO_4)_4$ (JCPDS file no. 12-399) [4–6] or $ThO_2 \cdot 0.8\ P_2O_5$ (JCPDS file no. 31-1388) [7] were wrongly identified or do not exist. They must be replaced by the thorium phosphate–diphosphate (TPD): $Th_4(PO_4)_4P_2O_7$ (namely TPD; JCPDS file no. 86-669) which was synthesized either by wet or dry chemistry methods [8,9], then characterized [10].

The aim of this study consisted in the immobilization of ^{239}Pu ($\alpha, T_{1/2} = 24\,500$ yr) and its daughter ^{235}U ($\alpha, T_{1/2} = 7.04 \times 10^8$ yr) or of ^{241}Pu ($\beta^-, T_{1/2} = 14$ yr) and its daughters, i.e., ^{241}Am ($\alpha, T_{1/2} = 432.2$ yr) and ^{237}Np ($\alpha, T_{1/2} = 2.14 \times 10^6$ yr) and the final disposal needed for the excess of plutonium from dismantled nuclear weapons. Thus, we verified that the replacement of Th^{4+} by large amounts of smaller tetravalent actinides like U^{4+}, Np^{4+} or Pu^{4+} was possible in the TPD structure [11,12]. It was obtained up to 75 mol% by uranium (IV), up to 52 mol% by neptunium (IV) and up to 41 mol% by plutonium (IV) leading to the formation of solid solutions of formula $Th_{4-x}M_x(PO_4)_4P_2O_7$ (with M = U, Np or Pu).

* Corresponding author. Tel.: +33-1 69 15 73 42; fax: +33-1 69 15 71 50.
E-mail address: dacheux@ipno.in2p3.fr (N. Dacheux).

0022-3115/00/$ - see front matter
PII: S0022-3115(00)00391-3

Moreover, in the case of the use of this material for the immobilization of actinides, it is necessary to evaluate its resistance to aqueous corrosion in order to give information about its long-term behavior in the environment. In fact, for deep underground disposal storage, water, which could be in contact with the container is one of the main vectors for the nuclides migration. For this reason, the dissolution mechanism of such a compound must be understood. Under these conditions, we performed several leaching experiments in order to study the influence of several parameters on the TPD dissolution. Owing to the very high resistance of the TPD to aqueous corrosion, several leaching tests were achieved in very corrosive media, varying surface, temperature, phosphate concentration and leaching flow. We also studied the influence of the acidity or basicity of the leachate on the normalized leaching (or dissolution) rate. The characterization of the solid when the saturation of the solution is reached was obtained considering either over- or under-saturation conditions.

2. Experimental

2.1. Chemicals and apparatus

The thorium nitrate solution was prepared by dilution of a concentrated solution ($C = 1.8$ M) purchased by Rhône Poulenc (La Rochelle, France). All the other chemicals used (phosphoric or nitric acid, sodium nitrate or perchlorate) were from Merck, Prolabo or Fluka.

The high temperature treatments were performed in a Pyrox HM 40 furnace in alumina boats up to 1050–1250°C with heating rates equal to 2–5°C min^{-1}.

The X-ray powder diffraction diagrams were collected with a Philips PW 1050/70 diffractometer using Cu K_α rays $\lambda = 1.5418$ Å from 10° to 60° (2θ) each 0.01° with an acquisition time equal to 0.3 s $step^{-1}$.

The electron probe microanalyses (EPMA) were carried out with a Cameca SX 50 apparatus using an acceleration voltage of 15 kV and a current of 10 nA. The diameter of the analytical spot was about 1 μm. The following calibration standards were used: ThO_2 (M_α ray of thorium) and $Ca_5(PO_4)_3OH$ (K_α ray of phosphorous).

The infrared spectra were recorded using a Hitachi I-2001 spectrophotometer (4000–400 cm^{-1}). The samples were ground in KBr (2–3 wt%) then pressed at 200–500 MPa.

The granulometric study was performed with a Coulter LS granulometer, while the specific surface area was determined with a Coulter SA 3100 apparatus using the BET method with nitrogen adsorption.

Polytetrafluoroethylene (PTFE) containers were chosen for the leaching experiments at 90°C, while for room temperature experiments, the containers were in high density polyethylene (HDPE). We verified that, in these conditions, less than 1% of the total dissolved elements is adsorbed onto the surface of the containers.

The thorium concentration was determined by α-liquid scintillation using the photon electron rejecting alpha liquid scintillation (PERALS) spectrometer marketed by Ordela (Oak Ridge, TN, USA) as already reported [13].

The TEM investigation was performed using either a Philips EM 400 or a Philips CM 12 electron microscope, both being equipped with high resolution stages (Supertwin for CM12) on samples which were prepared using hypercritical drying for hydrated compounds to preserve the texture of the hydrated phase. After drying, the samples were finally ground using a boron carbide mortar to obtain a fine powder (thickness less than 80 nm). All the TEM modes were used: bright field (BF), dark field (DF), selected area diffraction (SAD), nanodiffraction (ND) and lattice fringes (LF). The dark field mode was used following the principle of azimuthal and radial exploration of the reciprocal space, as more extensively described by Oberlin et al. [14]. An aperture was used in the back focal plane of the objective lens to select only some specific hkl beams to build the image. This allowed obtaining selective images of the leached TPD. Taking into account the width (1.9 nm^{-1} in the reciprocal space) and the location of the objective aperture (2.5 nm^{-1}), the DF position admits beams scattered in the 1.15–3.05 nm^{-1} range. In the normal space, DF potentially revealed planes between 0.87 and 0.328 nm, respectively. The radial exploration made possible the determination of the presence (or lack) of isotropy and the degree of crystallinity of phases from well-crystallized to amorphous. For amorphous compounds, the material always appear softly illuminated for all the radial positions (0°, 45°, 90°), while crystals (under Bragg conditions) appear white for one position and dark for the others. For amorphous materials, the size bright dots led at zero, while it led up to crystallite size for crystalline materials [15]. ND mode supposed that only the incident beam is used to get diffraction pattern from the sample. The effective size, which contributes to the diffraction pattern, is that illuminated by the beam. The effective spatial resolution was directly monitored by the beam size in parallel mode, which is inferior to 100 nm of diameter in this study. LF mode was allowed resolving the structural periodicity of the crystalline specimens. To obtain such images, it was necessary to select more than one beam with an appropriate objective diaphragm. In this case, the incident beam and a diffraction beam were selected to get the phase contrast image, which revealed the periodicity of the specimen. In fact, more than two beams were selected due to the large number of diffracted beams existing in the TPD and selected by the diaphragm objective (all the hkl line between 2 and 0.25 nm in our experimental conditions).

2.2. Synthesis of TPD

In our previous publications, we already reported several ways of synthesis of the TPD based on wet and dry chemical methods [8–10]. This compound can be synthesized after heating at high temperature (1100–1350°C) in air or under inert conditions, whatever the chemical way of synthesis, whatever the thorium salt used (thorium nitrate, chloride, bromide, oxalate, oxide ...) and the phosphating reactant (phosphoric acid, ammonium hydrogenphosphate ...) provided that the initial mole ratio $r = Th/PO_4$ is equal to 2/3. The solid obtained after heating is always a well-crystallized, homogenous and single phase. For all the other mole ratios r, the system is polyphase after heating at 1250°C. It is composed of TPD and ThP_2O_7 (JCPDS file no. 17-576) for $r < 2/3$ and of TPD and ThO_2 (JCPDS file no. 42-1462) or $(ThO)_3(PO_4)_2$ (JCPDS file no. 16-805) for $r > 2/3$.

For performing the leaching experiments, several grams of TPD were prepared from a mixture of concentrated thorium nitrate (1.5–2.1 M) and phosphoric acid (5 M) solutions. This mixture was slowly evaporated between 100°C and 200°C, then ground and heated, first at 400°C for 2–5 h in air or under inert conditions (Ar) in alumina boats in order to get the evaporation of volatiles. The solid was thus heated up to 1250°C for 10 h with a heating rate equal to 3–5°C min^{-1}.

2.3. Characterization

The ab initio structure determination was performed on powdered TPD and on single crystal (JCPDS file no. 86-669). An orthorhombic unit cell was found (space group *Pcam*, $Z = 2$) with $a = 12.8646(9)$ Å, $b = 10.4374(8)$ Å and $c = 7.0676(5)$ Å. In this structure, the thorium atoms are eightfold coordinated. The coexistence of mono- and diphosphate groups in the same material was confirmed using IR and Raman spectroscopies. The mole ratio $r = Th/PO_4$ was verified by EPMA. The results are in very good agreement with the values calculated considering the general formula $Th_4(PO_4)_4P_2O_7$ (Table 1). Indeed, for powdered and sintered samples, the mole ratios as well as the elementary wt% are consistent with the general formula. After grinding, the grain size was spread from 1 to 40 μm with an average value of 10 μm. The corresponding specific surface area of the powder reached 0.2–0.4 $m^2\ g^{-1}$.

Table 1
EPMA analysis of unleached TPD samples

Wt%	Calc.	Exp. (powdered TPD)	Exp. (sintered TPD)
Th	62.6	62.6 ± 0.5	63.1 ± 0.7
P	12.6	12.6 ± 0.3	12.3 ± 0.2
O	24.8	24.8 ± 0.3	24.6 ± 0.3
Total	100	100.0 ± 1.1	100.0 ± 1.2
Th/P	0.667	0.667 ± 0.013	0.685 ± 0.009

2.4. Sintering

Sintered samples of TPD were obtained from the residue prepared by the complete evaporation of the solution then heating treatment at 400°C during 2 h as previously described in the previous section. This precursor was firstly shaped into pellet form via a uniaxial room temperature pressing at 100–800 MPa. It was thermally treated at 400°C for 2 h, then up to 1250°C for 10 h with a heating rate equal to 2–5°C min^{-1}. The variations of the sample density and the shrinkage were determined in terms of the initial pressure used. The density measurements were performed using helium, xylene and water pycnometries in order to verify that no problem concerning the penetration of the solvent in the solid occurred in our experimental conditions. For water experiments, which was the main way of density determination used, we determined either the effective or the apparent density to evaluate the open and closed porosities. From 200 to 800 MPa, the density of the pellets obtained varied from 95% to 99% of the calculated value ($d_{calc} = 5.19$) while the shrinkage decreased from almost 15% to 10%. When pressing at 500 MPa, the corresponding open and closed porosity decreased from 8% and 4%, respectively after heating for 10 h to 3% and 2%, respectively, when the heating treatment was continued up to 120 h. The complete characterization of the pellets obtained will be published soon [16].

2.5. Leaching tests procedure and analysis of the leachate

Since the TPD dissolution is very slow, several leaching tests were achieved in a very corrosive media at constant temperature for several months in order to increase the dissolution rate and to put in evidence the formation of neoformed phases. For each dissolution experiment, samples of 50 mg to 1.4 g of powdered or ceramized TPD were put into 5 ml of 5 M HNO_3 and shaken for several days to few months. Both phases were thus separated by centrifugation at 2000 rpm. A part of the leachate was then taken off and analyzed. This volume was renewed with fresh concentrated nitric acid.

For experiments using several leaching flows (from 0.02 to about 20 ml $m^{-2}\ d^{-1}$), an aliquot of 100 μl to 3ml of the leachate was taken off then renewed with fresh solution at regular intervals. For all the other experiments, only 2% of the leachate were taken off, in order to avoid any perturbation of the solid solution system (they corresponded to a leaching flow equal to 0.5 ml $m^{-2}\ d^{-1}$).

The thorium activity released in the solution was measured by α-liquid scintillation (PERALS® spectrometry) using a liquid–liquid extraction step in 1 M HNO_3 by the di-2-ethyl-hexyl phosphoric acid (this extractive molecule is contained in ALPHAEX™). In these conditions, the thorium recovery reached 97–100% for a volume ratio between organic and aqueous phases equal to 0.25 [13].

Owing to very corrosive conditions, the dissolution rates were calculated for short periods making the assumption that during this leaching time, the mass and the surface of the solid were unchanged and that no neoformed phases were obtained by over-saturation. In fact, the specific surface area is not constant during the leaching tests but Östhols et al. [17] pointed out that this assumption can be used since a loss of the mass of solid and an increase of the porosity give opposite effects on the surface area. We calculated the normalized leaching rates from the quantity of dissolved thorium considering that the dissolution of the solid is congruent which was verified afterwards for all the conditions studied.

Moreover, a higher release was initially observed because of the surface heterogeneity of unwashed minerals (minor phases, non-stoichiometry at the surface, particle size inferior to 1 μm, ...). Nevertheless, considering the very corrosive medium we used, the surface irregularities were rapidly eliminated and, by this way, no significant increase was noted at the beginning of the dissolution curves. All these problems were avoided by the washing step.

3. Theoretical section

3.1. Dissolution theory

Several studies dealt with the dissolution of minerals especially in the case of weathering conditions. According to the theory, the rate of a chemical reaction is controlled by the decomposition of an activated complex [18]. Many authors already extended this approach in order to explain the dissolution of minerals from a kinetic point of view. Thus, initial attempts to explain the dissolution kinetics involved the transition state theory [19], while a second approach, developed by Stumm et al. [20,21], was based on the coordination chemistry. Other authors used a combination of both approaches [22,23] or considered a more general law in which all the parameters are macroscopic [24,25]. All these authors agreed that for most of the minerals, the dissolution rate is controlled by surface reactions at the solid–solution interface with the decomposition of an activated complex. Furthermore, most heterogeneous reactions involve the following steps:

- adsorption of aqueous species onto the surface;
- reaction of adsorbed species among themselves or with atoms of the surface;
- desorption of the product species formed at the surface.

A rigorous application of the rate law determined from the transition state theory is only possible for elementary reactions which makes this rate law difficult to apply to overall dissolution reactions. In these conditions, we were especially interested in the approach developed by Lasaga et al. [25].

3.2. Definitions and expression of the normalized leaching (or dissolution) rate

The leachability of the element i from a mineral (in our case, i is one of the elements contained in the TPD, i.e., usually thorium or phosphorous) can be described by its normalized leaching, $N_L(i)$ (g m^{-2}) which is defined by the relation

$$N_L(i) = \frac{\Delta m_{i\,\mathrm{sol}}}{f_i S} = \frac{m_i}{f_i S}, \tag{1}$$

where m_i corresponds to the total amount of i measured in the solution (g), S the corresponding solid area (m^2) and $\Delta m_{i\,\mathrm{sol}}$ corresponds to the mass loss of i in the solid

$$\Delta m_{i\,\mathrm{sol}} = m_{i\,\mathrm{sol},0} - m_{i\,\mathrm{sol},t} = m_i. \tag{2}$$

In this equation, $m_{i\,\mathrm{sol},0}$ is the initial mass of i in the solid, $m_{i\,\mathrm{sol},t}$ the mass of i in the solid after a leaching time equal to t and f_i is the mass ratio of the element i in the solid, i.e.,

$$f_i = \frac{m_{i\,\mathrm{sol},0}}{m_{\mathrm{sol}}}, \tag{3}$$

where m_{sol} represents the total mass of the solid.

Derivating Eq. (1) as a function of time, the normalized leaching rate of the element i can be written as

$$\frac{\mathrm{d}N_L(i)}{\mathrm{d}t} = \frac{1}{f_i S}\frac{\mathrm{d}m_i}{\mathrm{d}t}. \tag{4}$$

The normalized leaching rate corresponds to the slope obtained from the linear regression of the variation of the normalized leaching versus time as it was mentioned by several authors for washed minerals [26–28]. A higher release was initially observed because of the surface heterogeneity of unwashed minerals (minor phases, non-stoichiometry at the surface, particle size inferior to 1 μm, ...). As already described in the experimental section, these artifacts were canceled by the washing step in corrosive media.

From Eq. (1), we can also define the normalized leaching of the matrix as follows:

$$N_L = \frac{\Delta m_{\mathrm{sol}}}{S} = \frac{m}{S} = \sum_i f_i N_L(i), \tag{5}$$

where Δm_{sol} represents the mass loss of the solid and m is the mass of solid dissolved.

By derivating Eq. (5) as a function of time, we can write

$$\frac{dN_L}{dt} = \frac{1}{S}\frac{dm}{dt}. \quad (6)$$

In the case of a congruent dissolution, dm/dt can be directly determined from the mass loss of one of the components of the mineral, dm_i/dt, since

$$\frac{dm}{dt} = \frac{1}{f_i}\frac{dm_i}{dt}. \quad (7)$$

Thus, for a congruent dissolution, the normalized leaching (or dissolution) rate of the solid (g m^{-2} d^{-1}) can be written

$$R_L = \frac{1}{f_i S}\frac{dm_i}{dt} = \frac{dN_L(i)}{dt}, \quad (8)$$

where $dN_L(i)/dt$ corresponds to the derivative of Eq. (1) versus time which is equal to dN_L/dt whatever the element i considered when the dissolution is congruent.

3.3. Influence of the surface on the apparent dissolution rate

The reactive surface area is a fundamental variable in any kinetic of heterogeneous reaction. In the given conditions, the apparent dissolution rate of a mineral, r (g d^{-1}), is expressed with the general law [24]

$$r = \frac{dm}{dt} = R_L S, \quad (9)$$

where dm/dt corresponds to the derivation of the mass of mineral dissolved and R_L represents the leaching rate of the solid (g m^{-2} d^{-1}).

3.4. Influence of temperature on the normalized leaching rate

Temperature is also a main parameter affecting the normalized leaching rate according to the Arrhenius law, i.e.,

$$R_L = k e^{(-E_{app}/RT)}, \quad (10)$$

where k is the dissolution rate constant independent of the temperature (g m^{-2} d^{-1}) and E_{app} is the apparent activation energy of the dissolution of the mineral (kJ mol^{-1}).

As the temperature dependence of the dissolution rate law for the overall dissolution may be more complex than the temperature dependence of an elementary reaction, the terminology of apparent activation energy was used to make the difference with the classical activation energy [25]. The apparent activation energy could result from the contribution of the enthalpy of proton adsorption in order to form the activated complex. Thus, this contribution could slightly depend on the pH [29]. Furthermore, detailed molecular theories often yield to a temperature dependent activation energy and pre-exponential factor k [29]. This weak dependence was experimentally determined with difficulty and so the Arrhenius equation mentioned in Eq. (10) was considered as a reasonable approach. When the variation of $\ln(R_L)$ is plotted as a function of the reciprocal temperature, Eq. (10) leads to

$$\ln(R_L) = \ln k - \frac{E_{app}}{RT}. \quad (11)$$

3.5. Influence of pH on the normalized leaching rate

Many authors already investigated the influence of pH on the normalized leaching rate. They showed that the normalized leaching rates of most of the minerals increase with the proton activity for pH < 7. Under acidic conditions, the experimental dissolution rate of many minerals [22,23,30–32] and of the doped TPD [33,34] was found to be proportional to a fractional power of the proton activity. The notation usually used for normalized leaching rate is R_H in acidic media and R_{OH} in basic media.

In this case, Eq. (10) leads to

$$R_H = k'(a_{H_3O^+})^n \exp\left(-\frac{E_{app}}{RT}\right), \quad (12)$$

where R_H refers to the proton-promoted dissolution rate (g m^{-2} d^{-1}) and k' is the apparent normalized dissolution rate constant for proton-promoted dissolution defined for pH < 7 and independent of pH (g m^{-2} d^{-1}). The $a_{H_3O^+}$ corresponds to the proton activity and n represents the partial order related to the proton ions.

When the temperature is kept constant, it is easier to consider the following relation:

$$R_H = k'_T(a_{H_3O^+})^n. \quad (13)$$

In this equation, k'_T corresponds to the normalized dissolution rate constant for proton-promoted dissolution. k'_T is defined for pH < 7. It is independent of pH, but dependent on temperature and expressed in g m^{-2} d^{-1}.

For several minerals, the partial order related to the proton activity was fractional and found to be between $0 < n < 1$ [32]. We must note that even if this order depends on the dissolution mechanism, it does not correspond to the number of protons involved in the dissolution reaction. Some authors tried to interpret this fractional dependence in terms of concentrations (or activities) of species at the surface of the solid [21,32,35]. They found an integer partial order related to the adsorbed protons onto the surface. However, this number

seems to be interpreted differently. Indeed, other authors used the hypothesis of the regular solid solution behavior for the formation of the activated complex on the sample surface [22,36]. They interpreted the fractional order, as the ratio of the stoichiometric coefficient for protons in the formation of an activated complex, with a number related to the excess enthalpy of mixing of the solid solution. In both cases, the influence of pH on the normalized dissolution rate can be explained by the decomposition of an activated complex whose concentration at the surface depends on the proton concentration in the leachate. The previous relation implies the proton activity. Nevertheless, in most of the cases, it is easier to use the proton concentration. Introducing the proton activity coefficient, Eq. (13) becomes

$$R_{\mathrm{H}} = k'_{\mathrm{T}}(\gamma_{\mathrm{H_3O^+}}[\mathrm{H_3O^+}])^n = k'_{\mathrm{T},I}[\mathrm{H_3O^+}]^n, \tag{14}$$

with

$$k'_{\mathrm{T},I} = k'_{\mathrm{T}}(\gamma_{\mathrm{H_3O^+}})^n. \tag{15}$$

In this expression, $k'_{\mathrm{T},I}$ represents the apparent normalized dissolution rate constant for proton-promoted dissolution defined for pH < 7 and $\gamma_{\mathrm{H_3O^+}}$ corresponds to the proton activity coefficient. $k'_{\mathrm{T},I}$ is independent of the pH, but dependent on the temperature, the medium and the ionic strength I.

Several authors have also studied the influence of pH on the dissolution of the mineral in basic media. They showed a partial order related to the hydroxide ions similar to that related to the proton ions [21,22] and established the relation

$$R_{\mathrm{OH}} = k''_{\mathrm{T}} \times (a_{\mathrm{OH^-}})^m, \tag{16}$$

k''_{T} represents the normalized dissolution rate constant for hydroxide-promoted dissolution defined for pH > 7. It is independent of pH and dependent on temperature. a^-_{OH} is the hydroxide ion activity and m the partial order related to the hydroxide ions.

As it was already mentioned for the partial order n, the m values reported in the literature are usually between 0 and 1. Furthermore, it is easier to use the expression of the normalized leaching rate in terms of the hydroxide ions concentration. It can be written

$$R_{\mathrm{H}} = k''_{\mathrm{T}}(\gamma_{\mathrm{OH^-}}[\mathrm{OH^-}])^m = k''_{\mathrm{T},I}[\mathrm{OH^-}]^m, \tag{17}$$

with

$$k''_{\mathrm{T},I} = k''_{\mathrm{T}} \times (\gamma_{\mathrm{OH^-}})^m. \tag{18}$$

In this expression, $k''_{\mathrm{T},I}$ is the apparent normalized dissolution rate constant defined for pH > 7 and $\gamma_{\mathrm{OH^-}}$ represents the hydroxide ion activity coefficient. $k''_{\mathrm{T},I}$ is independent of the pH but dependent on the temperature, the medium and the ionic strength I.

3.6. Influence of the phosphate concentration on the normalized leaching rate

The TPD dissolution could also be influenced by the phosphate concentration. The role of the phosphate ions is important because they are involved in the TPD constitution and probably in that of the activated complex formed at the surface of the solid. This observation implies that the presence of the phosphate ions could enhance the TPD dissolution by increasing the concentration of the activated complex. Owing to the acido-basic properties of the phosphate ions, their effect on the normalized leaching rate could be dependent on the pH. In these conditions, Eq. (13) can be written

$$R_{\mathrm{H}} = k'_{\mathrm{T}}[1 + b(a_{\mathrm{PO_4}})^p](a_{\mathrm{H_3O^+}})^n, \tag{19}$$

where $a_{\mathrm{PO_4}}$ represents the phosphate activity, b a constant and p is the partial order related to the total phosphate ions present in the leachate. In terms of the phosphate concentration, Eq. (19) leads to

$$R_{\mathrm{H}} = k'_{\mathrm{T}}[1 + b(\gamma_{\mathrm{PO_4}})^p(\mathrm{C_{PO_4}})^p](\gamma_{\mathrm{H_3O^+}})^n[\mathrm{H_3O^+}]^n, \tag{20}$$

which can be written

$$R_{\mathrm{H}} = k''_{\mathrm{T},I}[1 + b_I(\mathrm{C_{PO_4}})^p][\mathrm{H_3O^+}]^n, \tag{21}$$

with

$$b_I = b(\gamma_{\mathrm{PO_4}})^p. \tag{22}$$

b_I is a constant dependent on the medium and on the ionic strength.

4. Results and discussion

4.1. Kinetic study of the TPD dissolution

4.1.1. Influence of the surface on the apparent dissolution rate

If the TPD dissolution is congruent (i.e., stoichiometric and without any neoformed phase), the apparent dissolution rate of the mineral should be linearly dependent on the sample surface area (Eq. (9)). We verified this relation by performing leaching tests as a function of the surface of the solid. Powdered samples of TPD were mixed with concentrated nitric acid (5 M HNO_3) at room temperature considering several mass of the solid (50 mg to 1.4 g) with various surface area. We measured the amount of dissolved thorium, then determined the apparent leaching rate $\mathrm{d}m/\mathrm{d}t$ as a function of S making the assumption that the TPD dissolution is congruent which was verified for pH $\leqslant 1$ as verified in Section 4.2.2.

As shown in Fig. 1 and in Table 2, the relation between $\mathrm{d}m/\mathrm{d}t$ and S is perfectly linear. This linear relation confirms that, in these operating conditions, the species measured in the solution are under-saturation

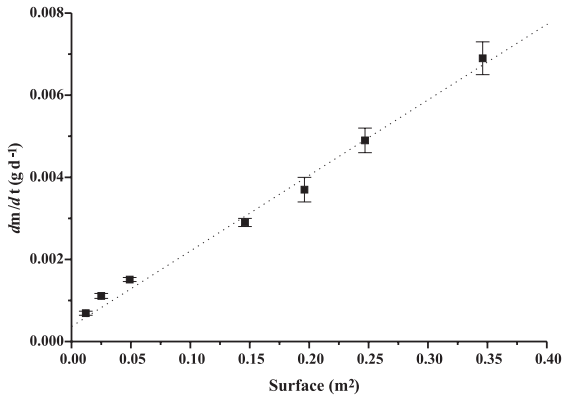

Fig. 1. Variation of $r = \mathrm{d}m/\mathrm{d}t$ as a function of the surface area S (5 M HNO_3, 25°C).

Table 2
r dependence on the surface area for TPD (5 M HNO_3, 25°C)

Surface (m^2)	$r = \mathrm{d}m/\mathrm{d}t$ (g d^{-1})
0.012	$(6.9 \pm 0.3) \times 10^{-4}$
0.025	$(1.11 \pm 0.07) \times 10^{-3}$
0.049	$(1.51 \pm 0.06) \times 10^{-3}$
0.146	$(2.9 \pm 0.1) \times 10^{-3}$
0.196	$(3.7 \pm 0.3) \times 10^{-3}$
0.247	$(4.9 \pm 0.2) \times 10^{-3}$
0.346	$(6.9 \pm 0.3) \times 10^{-3}$

conditions. Thus, secondary phases are not formed during the first days of dissolution. The regression of the straight line obtained leads to

$$r = \frac{\mathrm{d}m}{\mathrm{d}t} = 1.84(8) \times 10^{-2} S + 3(1) \times 10^{-4}. \quad (23)$$

Considering this equation, the slope corresponds to the R_H value obtained in 5 M HNO_3 at 25°C (Eq. (9)). This value is in very good agreement with the value reported in Table 4 for these operating conditions ($R_H = 1.93(8) \times 10^{-2}$ g m^{-2} d^{-1} at 25°C). The intercept value is near to zero, which is coherent with Eq. (9).

Another study was performed in order to compare the dissolution curves of powdered and ceramized samples whose specific surface area are very different. Both TPD samples were mixed at 90°C with 5 M HNO_3 in the same conditions. The dissolution rates were found to be equal to $2.5(3) \times 10^{-3}$ and 0.14(1) g d^{-1} for sintered and powdered samples, respectively. From this study, it appears that the apparent dissolution rate is dependent on the surface of the sample, which is in good agreement with the study mentioned above.

4.1.2. Influence of the leaching flow on the normalized leaching rate

The effect of the leaching flow was studied in order to confirm that no secondary phase was precipitated during the leaching tests. These tests were performed using 200 mg of TPD and 5 ml of 5 M HNO_3 at room temperature for leaching flows varying from 0.02 to 20 ml m^{-2} d^{-1}. As already mentioned, the normalized leaching rates were determined considering that the dissolution of the TPD is stoichiometric which was verified for all the media studied. The normalized leaching is presented in Fig. 2 for each leaching flow considered. The corresponding normalized leaching rates are gathered in Table 3. The results obtained showed that the normalized dissolution rate remains almost constant when increasing the leaching flow during the first 50 days of leaching time. This confirms that no secondary phase was formed for these operating conditions.

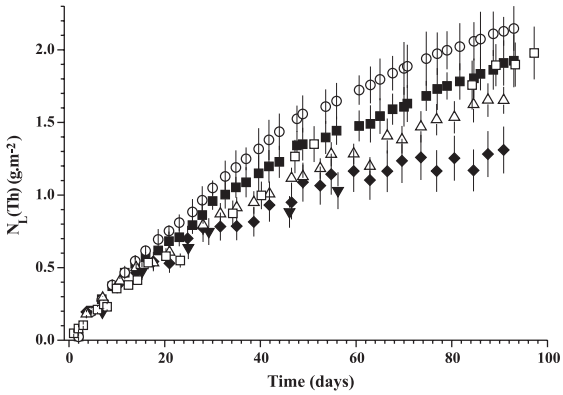

Fig. 2. Evolution of N_L(Th) for several leaching flows in 5 M HNO_3 at 25°C (○ 20 ml m^{-2} d^{-1}; ■ 7 ml m^{-2} d^{-1}; △ 2.0 ml m^{-2} d^{-1}; □ 0.6 ml m^{-2} d^{-1}; ◆ 0.4 ml m^{-2} d^{-1}; ▼ 0.02 ml m^{-2} d^{-1}).

Table 3
R_H dependence on the leaching flow for TPD (5 M HNO_3, 25°C)

Leaching flow (ml m^{-2} d^{-1})	R_H (g m^{-2} d^{-1})
0.02	$(2.4 \pm 0.1) \times 10^{-2}$
0.4	$(2.7 \pm 0.2) \times 10^{-2}$
0.6	$(2.7 \pm 0.1) \times 10^{-2}$
2.0	$(3.1 \pm 0.1) \times 10^{-2}$
7	$(3.6 \pm 0.1) \times 10^{-2}$
20	$(3.8 \pm 0.1) \times 10^{-2}$

Table 4
R_H dependence on the temperature for TPD (5 M HNO_3)

Temperature (K)	R_H (g m^{-2} d^{-1})
277	$(4.5 \pm 0.1) \times 10^{-3}$
298	$(1.93 \pm 0.08) \times 10^{-2}$
323	$(5.3 \pm 0.1) \times 10^{-2}$
343	$(2.5 \pm 0.3) \times 10^{-1}$
363	$(4.0 \pm 0.3) \times 10^{-1}$
393	$(7.6 \pm 0.4) \times 10^{-1}$

4.1.3. Influence of the temperature on the normalized leaching rate

As reported in the theoretical section, the temperature is a main parameter affecting the normalized leaching rate (Eq. 10). For this reason, we studied the temperature dependence of the TPD normalized leaching rate. The apparent activation energy was determined from the slope of the straight line obtained when drawing the variation of $\ln(R_H)$ as the reciprocal temperature. Several leaching tests were performed for different temperatures (between 4°C and 120°C) keeping constant the surface/volume ratio (1.4 g of TPD – 5 ml of 5 M HNO_3; $S/V = 700$ cm^{-1}). The normalized leaching rates are gathered in Table 4, while the variation of $\ln(R_H)$ versus the reciprocal temperature is plotted in Fig. 3. The slope obtained from the linear regression led to an apparent activation energy equal to (42 ± 3) kJ mol^{-1}.

Leaching tests were also performed for $Th_{3.6}Pu_{0.4}(PO_4)_4P_2O_7$ in distilled water at room temperature and at 90°C in order to show if the E_{app} value depends on the leachate acidity. They led to $E_{app} = (41 \pm 1)$ kJ mol^{-1} which is in very good agreement with the value mentioned above. In these conditions, E_{app} seems to be independent of the acidity of the leachate. Moreover, both values are in good agreement with the apparent activation energy reported by several authors for other minerals since E_{app} was usually found between 40 and 80 kJ mol^{-1} [24] as reported in Table 5.

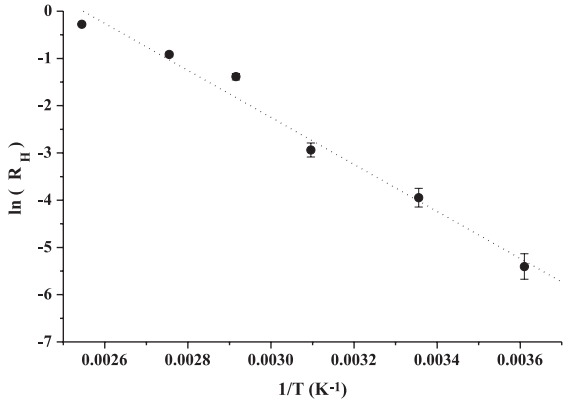

Fig. 3. Variation of $\ln(R_H)$ versus the reciprocal temperature (5 M HNO_3).

This value is higher than that expected for diffusion-controlled reactions (activation energy less than 21 kJ mol^{-1}) [43] which indicates that the dissolution is not controlled by solution-transport mechanism. The dissolution mechanism is also controlled by surface reactions as shown for most of the minerals studied. Furthermore, the activation energy of the TPD is smaller than the energy required for the breaking of a covalent bound (160–400 kJ mol^{-1}). The adsorption energy of surface species could have an important role in the decrease of the activation energy as already discussed by Lasaga et al. [25]. In fact, during chemical adsorption, the heat liberated is generally greater than 80 kJ mol^{-1}.

4.1.4. Influence of the acidity (or basicity) of the leachate on the normalized leaching rate

Owing to the precipitation of thorium for pH $\geqslant$ 1, we determined the influence of the pH on the normalized leaching rate for samples of TPD doped with small amounts of trivalent actinides (^{241}Am or ^{244}Cm) between pH = 1 and 3. The ionic strength was fixed to $I = 0.1$ M by addition of $NaClO_4$ or $NaNO_3$. The R_H values were measured for several pH (Table 6) and allowed the determination of the n and $k'_{298\ K,0.1\ M}$ values (Eq. (14)). The complete results concerning the dependence of R_H on the acidity or basicity of the leachate will be published soon in more detail [44]. The n value found between 0.31 and 0.35 is slightly lower than that reported for several other materials or minerals [22,32,45]. In these conditions, the TPD appears more resistant to the corrosion since its normalized leaching rates remain low even in very acidic media.

We also performed several leaching tests in basic media in order to determine the influence of hydroxide

Table 5
E_{app} values obtained for several minerals or materials

Mineral/material	E_{app} (kJ mol^{-1})	pH	Reference
Albite	71.6	1.4	[37]
Andalusite	48.1	1	[38]
Kaolinite	55.7	2	[39]
Microcline	52.3	3	[40]
Tephroite	54.0	2.5	[29]
PDT	42 ± 3	5 M HNO_3	This work
PDTP	41 ± 1	H_2O	This work
Zircon	23.2	12	[41]
Zirconolite	19–25	Not mentioned	[41]
Synroc	15–30	H_2O	[42]

Table 6
R_H dependence on the acidity of the leachate [44]

$[H_3O^+]$	TPD doped with ^{244}Cm – R_H (g m^{-2} d^{-1})[a]	TPD doped with ^{241}Am – R_H (g m^{-2} d^{-1})[b]
10^{-1} M	$(1.2 \pm 0.1) \times 10^{-5}$	$(5.9 \pm 0.1) \times 10^{-6}$
10^{-2} M	$(6.0 \pm 0.2) \times 10^{-6}$	$(1.84 \pm 0.04) \times 10^{-6}$
10^{-3} M	$(2.9 \pm 0.2) \times 10^{-6}$	$(1.18 \pm 0.04) \times 10^{-6}$
n	0.31 ± 0.01	0.35 ± 0.04
$k'_{298\ K,0.1\ M}$	$(2.4 \pm 0.1) \times 10^{-5}$	$(1.2 \pm 0.3) \times 10^{-5}$

[a] Leaching tests performed in $HClO_4$ and for $I = 0.1$ M.
[b] Leaching tests performed in HNO_3 and for $I = 0.1$ M.

ions concentration on the R_{OH} values. According to Eq. (17), we found a partial order related to the hydroxide concentration, m, equal to 0.35 ± 0.01 and a corresponding apparent normalized dissolution rate constant $k''_{298\ K,0.1\ M}$ equal to $6.6(1) \times 10^{-5}$ g m^{-2} d^{-1}. Thus, the resistance of TPD to the acidity (or basicity) of the leachate appears to be very good in all the media studied as it will be published soon [44].

4.1.5. Influence of the phosphate concentration on the normalized leaching rate

Several leaching tests were performed with 200 mg of TPD in 5 M HNO_3 at 25°C and for phosphate concentrations varying from 10^{-2} to 0.89 M in order to determine the partial order related to the phosphate ions p and the b_I constant value (Eq. (21)). The variation of the normalized leaching rate versus the total phosphate concentration (which is mainly present in the H_3PO_4 form in these operating conditions) is plotted in Fig. 4. The regression of the experimental results led to

$$R_H = 2.69 \times 10^{-2}[1 + 1.96 C_{PO_4}]. \quad (24)$$

According to Eq. (21), the b_I and p values are equal to 1.96(2) and 1.0, respectively. Furthermore, the straight line obtained gives an intercept equal to $2.69(3) \times 10^{-2}$ g m^{-2} d^{-1}. Since it corresponds to the proton-promoted dissolution rate in 5 M HNO_3 at 25°C in the absence of phosphate, this value is coherent with that deduced from the study of the leaching rates as a function of the surface area or temperature ($1.93(8) \times 10^{-2}$ g m^{-2} d^{-1}).

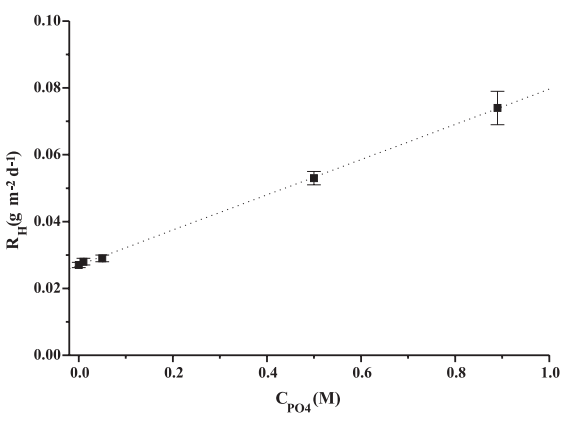

Fig. 4. Variation of R_H versus the phosphate concentration (5 M HNO_3, 90°C).

In conclusion, this study showed that phosphate ions are directly involved in the formation of the activated complex which is not surprising. Its concentration at the surface of the solid increases with the phosphate concentration in the leachate. That induces an increase of the normalized dissolution rate when increasing the phosphate concentration in the leachate. Nevertheless, the small b_I value found shows that the influence of phosphate on R_H remains very small. It becomes significant only for concentrations greater than 0.1 M. In fact, as the normalized dissolution rates of TPD for all the studies reported were determined considering short leaching times (less than 100 days), the total amount of dissolved phosphate remained always lower than 0.1 M. Thus, it was possible to neglect their influence on the R_H values reported previously.

4.2. Thermodynamic study of the TPD dissolution: observation and characterization of the neoformed phase

4.2.1. Dissolution curves

Leaching tests were continued at 90°C in order to obtain the complete dissolution of the TPD. The evolution of the dissolved mass of matrix was plotted for powdered and ceramized samples calculating the dissolved mass from the thorium content present in solution and its mass ratio in the TPD (Fig. 5). For both samples and for all leaching tests performed at several temperatures, two dissolution steps were observed:

- linear increase of the thorium content as a function of the leaching time;
- decrease of the dissolved thorium which reached a plateau.

The first part of the curve was observed during the first 4 and 20 days, respectively, for the powdered and the sintered TPD samples. For higher leaching times, the thorium content in solution strongly decreased then became constant after about 30 days. During this second step, the dissolved mass of TPD is not significant

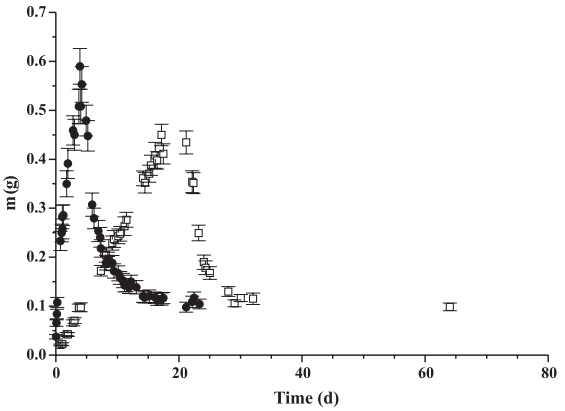

Fig. 5. Comparative evolution of m for powdered (●) and ceramized (□) samples (5 M HNO_3, 90°C).

because of the formation of a gelatinous-precipitate, which controls the thorium concentration in solution. The first dissolution step corresponds to a pure kinetic process. On the contrary, the second step is due to thermodynamic equilibrium in the leachate. In these conditions, the concentrations of dissolved species are in over-saturation conditions. Thus, they are controlled by the precipitation of a neoformed phase. For this reason, we focused the second part of our study on the complete characterization of the neoformed phase obtained when the saturation of the leachate was reached.

4.2.2. Characterization of the phase neoformed at the saturation of the solution

The solid obtained after the complete dissolution of the TPD was characterized by XRD. Its diffraction pattern (Fig. 6(b)) revealed diffraction lines, which did not overlap with those of the TPD (Fig. 6(a)). This analysis revealed that the TPD was completely dissolved during the leaching process, while a secondary phase partly crystallized was simultaneously formed. The SOCABIM search/match program was used for interrogating the ICDD PDF database [46] by constraining the search to thorium phosphates and thorium phosphates hydrates compositions. It was not possible to identify the neoformed phase to any compound mentioned in the literature. Moreover, the diffraction lines correspond to the thorium phosphate–hydrogen phosphate (TPHP) $Th_2(PO_4)_2(HPO_4)$, H_2O synthesized using hydrothermal conditions (Fig. 6(c)) [47].

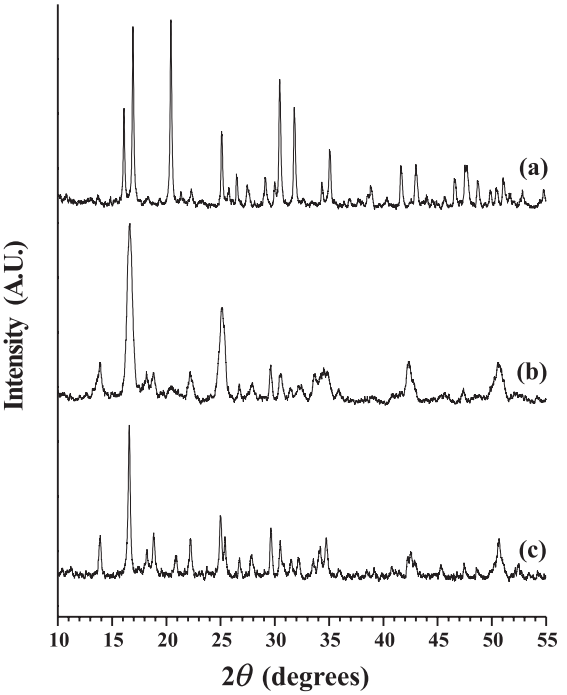

Fig. 6. XRD of unleached (a) and leached (b) TPD (5 M HNO_3, 90°C) – XRD of TPHP obtained using hydrothermal conditions (c).

The EPMA was performed on the samples obtained after the complete dissolution of TPD. The solids were analyzed after removal of the supernatant, on the one hand (Table 7, sample #1) or after the direct evaporation of the mixture at 90°C, on the other hand (Table 7, sample #2). In both cases, the wt% measured correspond to a mole ratio Th/P equal to 0.69 which is very close of the ratio $Th/PO_4 = 2/3$ found in the TPD. These

Table 7
EPMA analysis of leached TPD samples

Wt%	Calc.[a]	Exp. (#1)[b]	Exp. (#2)[c]	Exp. (#3)[d]
Th	62.6	52.7 ± 4.0	55.0 ± 2.2	54.6 ± 2.2
P	12.6	10.1 ± 0.8	10.7 ± 0.5	11.1 ± 0.8
O	24.8	20.3 ± 1.6	21.4 ± 0.8	22.0 ± 1.6
Total	100	83.1 ± 6.4	87.1 ± 3.5	87.9 ± 4.7
Th/P	0.667	0.694 ± 0.034	0.685 ± 0.023	0.657 ± 0.074

[a] calculated considering the formula $Th_4(PO_4)_4P_2O_7$.
[b] residue obtained after removal of the supernatant then evaporation at 90°C.
[c] residue obtained after the direct evaporation of the mixture at 90°C.
[d] solid obtained using hydrothermal conditions.

results are also in very good agreement with those obtained for the crystallized TPHP obtained from hydrothermal synthesis (Table 7, sample #3). Nevertheless, the total wt% is far from 100% which indicates that the solid also contains several water molecules.

It was confirmed by the observation of a broad strong band between 3500 and 2500 cm^{-1} in the infrared spectra recorded for the leached TPD (Fig. 7(a)). This band was assigned to the O–H stretching mode. Moreover, the band located near 1650 cm^{-1} is characteristic of the bending mode of H_2O. All the bands observed were attributed to the PO_4 bending and stretching modes as described in Table 8 by analogy with $U(UO_2)(PO_4)_2$ [48], $UClPO_4$, x H_2O [49] and $U_{1-x}Th_x(UO_2)(PO_4)_2$ [50]. On the contrary, the bands corresponding to the P–O–P stretching present in the P_2O_7 group is not observed in the IR spectrum of the leached TPD. Indeed, the stretching modes ν_s(P–O–P) and ν_{as}(P–O–P) were observed near 737 and 950 cm^{-1}, respectively, for α-ThP_2O_7 and α-UP_2O_7 [48]. Two bands are observed for the ν_s(P–O–P) stretching mode (707 and 734 cm^{-1}) and one for the ν_{as}(P–O–P) stretching mode (928 cm^{-1}) in the IR spectrum of TPD (Fig. 7(b)) [10].

The HPO_4^{2-} group can hardly be defined from the infrared spectra because of the overlap of (P)–O–H vibrations modes with those of O–H and P–O.

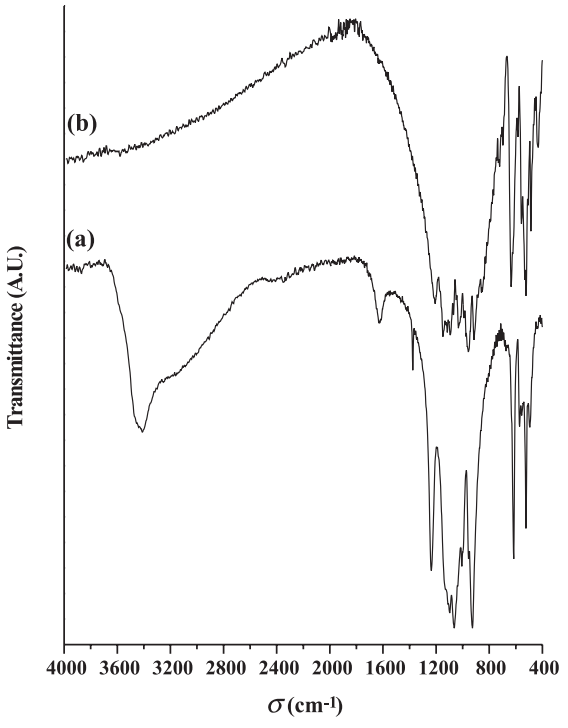

Fig. 7. IR spectrum of leached (a) (5 M HNO_3, 90°C) and unleached (b) TPD.

Table 8
Assignment of bands observed in the IR spectrum of TPHP

Frequency σ(cm^{-1})	Assignment
496	δ_s(P–O) of PO_4^{3-} and HPO_4^{2-}
522, 570, 616	δ_{as} (P–O) of PO_4^{3-} and HPO_4^{2-}
924	ν_s (P–O) of PO_4^{3-} and HPO_4^{2-}
1006–1096	ν_{as} (P–O) of PO_4^{3-} and HPO_4^{2-}
1234	ν_{as} ((P)–O–H) of HPO_4^{2-} (in the plane deformation [52])
1376	ν_{as} (N–O) of NO_3^- (adsorbed at the surface)
1620	H_2O bending mode
~2400 (shoulder)	ν_{as} ((P)–O–H) of HPO_4^{2-}
3600–3400 (broad)	H_2O stretching modes

Nevertheless, a weak shoulder at about 2400 cm^{-1} could be assigned to the (P)–O–H antisymmetric stretching mode as already reported for several hydrogen phosphate compounds [51,52]. The band observed at 1234 cm^{-1} can be also assigned to the (P)–O–H symmetric stretching mode in the plane deformation as reported in the literature [52].

In conclusion, all the techniques used aiming at the characterization of the phase neoformed when the TPD is totally dissolved lead to the proposed formula $Th_2(PO_4)_2(HPO_4)$, H_2O. In this solid, the mole ratio Th/P is equal to 2/3 which explains why, despite the precipitation of this phase, the ratio N_L(Th)/N_L(P) remains equal to 2/3 in leachate when the saturation of the solution is reached.

4.3. Observation of the TPD dissolution by TEM

The TEM analysis was performed either on unleached TPD and on the powder obtained after 1 and 219 days of leaching in 5 M HNO_3 at 90°C.

The LF and SAD micrographies of the unleached TPD (Fig. 8) show that the raw material is highly crystallized (grain size equal to several nm). Some grain-joints can be observed between two independent crystals. The corresponding (0 0 2) planes exhibit a 7° distorsion angle and save an open porosity (10 × 2.5 nm; white arrow). The SAD micrography is a powder type corresponding with sharp crystals randomly distributed. Some dots were indexed and assigned to several (hkl) diffraction planes of the TPD.

After 1 day of leaching in concentrated nitric acid, the leached TPD shows either on the bright field (Fig. 9(a)) and on the dark field (Figs. 9(b) and (c)) micrographies a typical trend of altered material. As shown from Fig. 9, a 20 nm thickness external layer around the fragments (black arrow) and corrosion pits of 4–5 nm average diameter (white arrow) are clearly visible. The two dark field micrographies correspond to

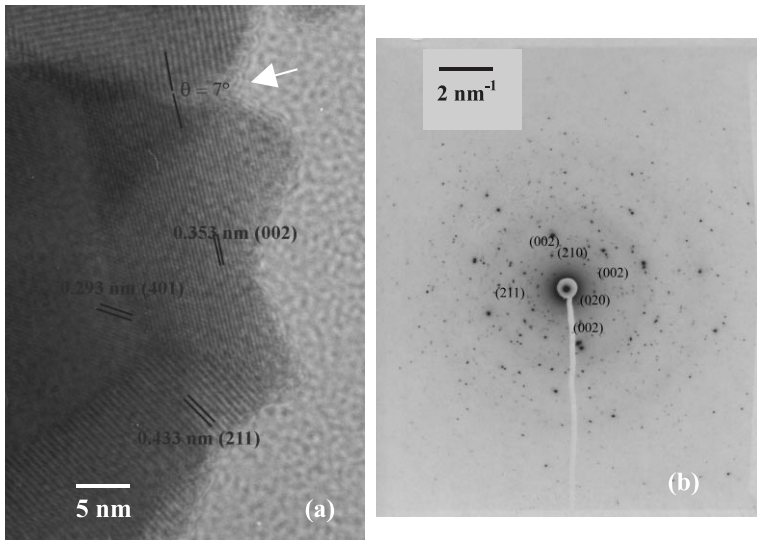

Fig. 8. Lattice fringes (a) and selected area diffraction (b) micrographies of the unleached TPD.

the 0° and 90° radial positions. The external layer keeps softly illuminated in grey colors which is characteristic of an amorphous structure. Thus, the leaching process of the TPD involves a corrosion mechanism, which leads to the formation of an amorphous layer at the solution-weathering solid interface.

A gelatinous phase was obtained when the leaching test was continued until the dissolution of TPD was almost complete (219 days of leaching tests in 5 M HNO_3 at 90°C). A TEM study was then achieved on the neoformed phase(s) after a hypercritical dessication procedure to preserve the texture of the hydrated phases. The bright field and nano-diffraction micrographies are reported in Fig. 10(a) and (b), respectively. From these figures, it clearly appears that the residue obtained is a polyphase system. The first phase is amorphous (white arrow) while the second one is well-crystallized (black arrow). The diffused ring (white arrow) is typical of the modulation induced by the defocused electron beam on a statistically disordered network of an amorphous structure. The indexation of the dots showed two different crystallized phases: the first one corresponds to the remaining TPD (Table 9), while the second one was identified as the crystallized TPHP which was also synthesized using hydrothermal conditions as already described.

Table 9
Nano-diffraction indexation for the remaining TPD

2R (cm)	d_{calc} (Å)	d_{exp} (Å)–XRD	hkl
1.03	7.019	7.067	0 0 1
1.12	6.455	6.443	2 0 0
1.82	3.973	3.968	3 1 0
2.15	3.363	3.359	1 3 0
2.34	3.090	3.074	4 1 0
2.46	2.939	2.927	4 0 1
2.61	2.770	2.738	4 2 0
3.04	2.378	2.3785	4 0 2
3.34	2.165	2.164	4 2 2
3.50	2.066	2.0602	1 5 0

5. Conclusion

The dissolution of TPD was systematically studied as a function of several parameters such as surface, leaching flow, temperature, acidity or basicity of the leachate and phosphate concentration. From the evolution of the normalized leaching of thorium, it was possible to determine the dependence of the normalized leaching rate of TPD on each parameter studied.

When the leachate is very corrosive (concentrated nitric acid), the absence of saturation of the solution was proved during the first days of leaching either by studying the influence of surface on the apparent dissolution rate or that of the leaching flow on the normalized leaching rate. In these conditions, the dependence of the normalized leaching rate on the temperature leads to an activation energy equal to about 42 ± 3 kJ mol^{-1}. It corresponds to mechanisms controlled by the surface reaction.

The presence of phosphate ions in the solution slightly increases the normalized leaching rate, but this increase is significant only for concentration higher than 0.1 M.

The acidity and the basicity of the leachate also increase the normalized leaching rate. The partial orders

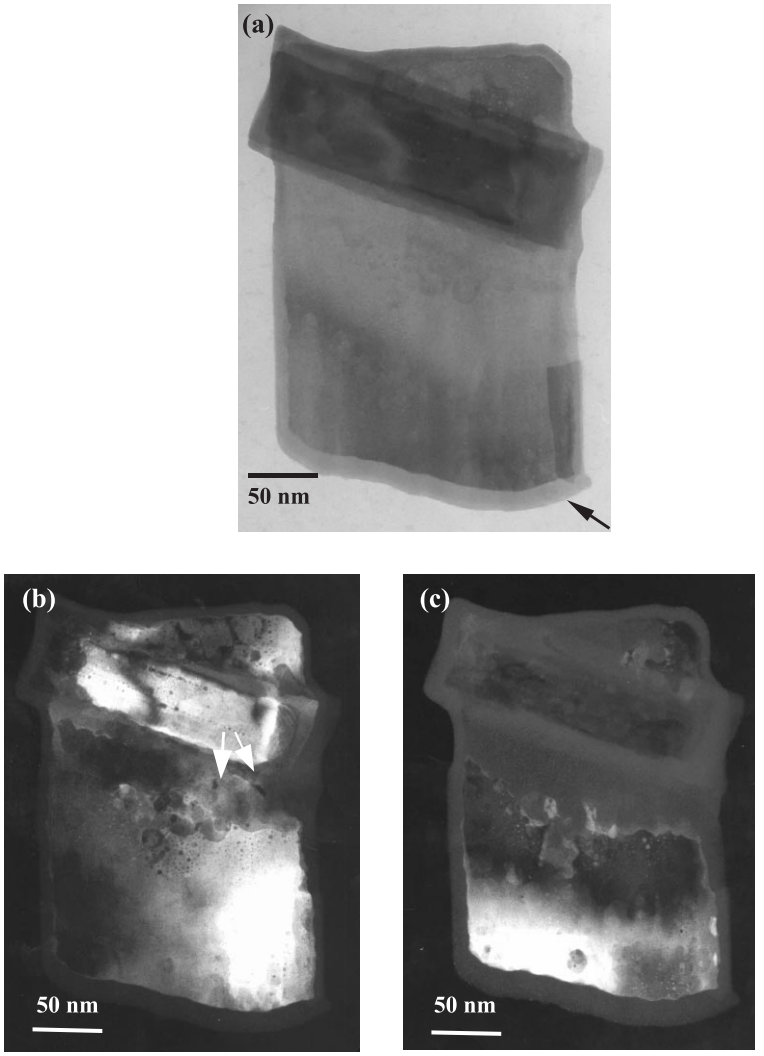

Fig. 9. Bright field (a) and dark field for 0° (b) and 90° (c) of the leached TPD (the black arrow shows the external layer and the white arrows indicate corrosion pits).

related to proton ions in acidic media and to hydroxide ions in basic media are quite similar: $n = 0.31$–0.35 for H_3O^+ and $m = 0.35$ for OH^-. The corresponding apparent normalized dissolution rate constant is in the 10^{-5} g m^{-2} d^{-1} range, which is very low. For $1 < pH < 4$ and $10 < pH < 13$, the normalized dissolution rate is always lower than 10^{-5} g m^{-2} d^{-1} which confirms the good retention properties of the TPD even in a very corrosive medium.

When the saturation of the solution is obtained, the neoformed phase was identified as the TPHP hydrate whose solubility product is very low ($K_S \approx 10^{-65}$) [44]. In these conditions, the thorium and phosphate concentrations measured in the leachate remain very low even (10^{-5} M) when the initial TPD is partly dissolved.

Simultaneously, the TEM study showed the formation of an amorphous external thin layer on the TPD surface and small corrosion pits during the first days of leaching in 5 M HNO_3. Several crystallized phases coexist inside the gel finally obtained after the rather complete dissolution of TPD.

From the experimental data reported in acidic and basic media, the normalized leaching rate calculated for pH = 7 and at 90°C reaches 3×10^{-6} g m^{-2} d^{-1}. For sintered TPD ($m = 1.4$ g), the corresponding leaching rate is thus equal to 7.5×10^{-8} g d^{-1}. In these conditions, the activity released in the leachate is equal to about 10^{-3}% of the solid one after 1 yr of leaching time, which remains very small by comparison to other materials such as apatites, monazites or zircons. As the

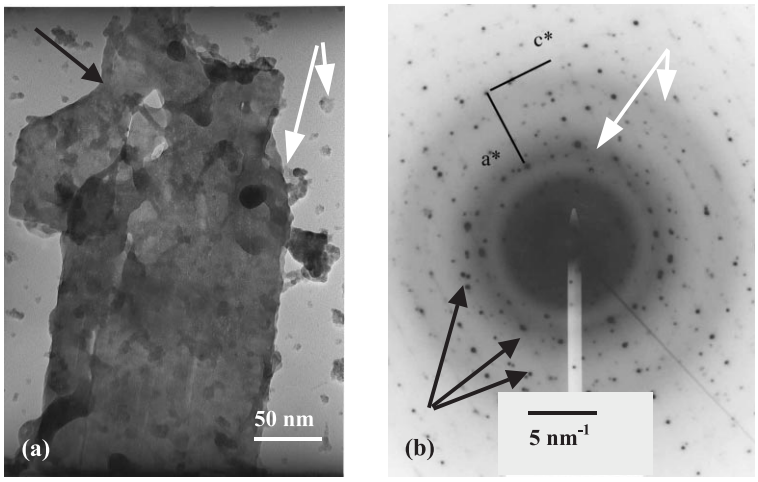

Fig. 10. Bright field (a) and nano-diffraction (b) of the hypercritical dried gel obtained from the leached TPD (the white and the black arrows show the amorphous and the crystallized phases, respectively).

normalized leaching rates of the TPD are always low, the migration of nuclides in water should be delayed from a kinetic point of view in the field of a deep underground repository. Moreover, the precipitation of neoformed phases containing phosphates (like TPHP) which are all low soluble should also delay the migration of nuclides for static conditions taking into account thermodynamic considerations. Both aspects show that the TPD could be used as a great advantage for the immobilization of actinides.

Several leaching tests were also performed on solid solutions $Th_{4-x}M_x(PO_4)_4P_2O_7$ (with M = U or Pu). For these solids, the normalized leaching rates remained low, while the precipitation of low soluble neoformed phases containing phosphates were put in evidence for each actinide studied. The main results obtained will be published soon and confirm the good retention properties of the TPD related to tetravalent and trivalent actinides.

References

[1] J. Carpena, F. Audubert, D. Bernache, L. Boyer, B. Donazzon, J.L. Lacout, N. Semanaud, Mater. Res. Soc. Symp. Proc. 508 (1998) 543.
[2] L.A. Boatner, B.C. Sales, in: W. Lutze, R.C. Ewing (Eds.), Radioactive Waste Forms for the Future, North-Holland, Amsterdam, 1988, p. 495.
[3] H.T. Hawkins, B.E. Scheetz, G.D. Guthrie, Mater. Res. Soc. Symp. Proc. 465 (1996) 387.
[4] A. Burdese, M.L. Borlera, Ann. Chim. Roma 53 (1963) 344.
[5] K.R. Laud, F.A. Hummel, J. Am. Ceram. Soc. 54 (1971) 296.
[6] J. Shankar, P.G. Khubchandani, Anal. Chem. 29 (1957) 1375.
[7] I.V. Tananaev, I.A. Rozanov, E.N. Beresnev, Inorg. Mater. (USSR) 12 (1976) 886.
[8] V Brandel, N. Dacheux, M. Genet, Radiokhim., in press.
[9] V. Brandel, N. Dacheux, E. Pichot, M. Genet, J. Emery, J.Y. Buzaré, R. Podor, Chem. Mater. 10 (1998) 345.
[10] P. Benard, V. Brandel, N. Dacheux, S. Jaulmes, S. Launay, C. Lindecker, M. Genet, D. Louër, M. Quarton, Chem. Mater. 8 (1996) 181.
[11] N. Dacheux, R. Podor, V. Brandel, M. Genet, J. Nucl. Mater. 252 (1998) 179.
[12] N. Dacheux, A.C. Thomas, V. Brandel, M. Genet, J. Nucl. Mater. 257 (1998) 108.
[13] N. Dacheux, J. Aupiais, Anal. Chem. 69 (1997) 2275.
[14] A. Oberlin, in: P.A. Thrown, M. Dekker (Eds.), Chemistry and Physics of Carbon, vol. 22, Dekker (Marcel), New York, 1989, p. 1.
[15] J.N. Rouzeau, A. Oberlin, M. Vandenbroucke, C.R. Somm, Soc. Géol. Fr. 5 (1978) 238.
[16] B Chassigneux, N. Dacheux, V. Brandel, M. Genet, G. Cizeron, to be published.
[17] E. Osthols, M. Malmström, Radiochim. Acta 68 (1995) 113.
[18] H. Eyring, J. Chem. Phys. 3 (1935) 107.
[19] P. Aagaard, H. Hegelson, Am. J. Sci. 282 (1982) 237.
[20] W. Stumm, G. Furrer, B. Kunz, Croat. Chem. Acta 56 (1983) 593.
[21] W. Stumm (Ed.), Chemistry of the Solid–Water Interface, Wiley, New York, 1992, p. 157.
[22] L. Chou, R. Wollast, Am. J. Sci. 285 (1985) 963.
[23] L. Chou, R. Wollast, J.I. Drever (Eds.), The Chemistry of Weathering, Reidel, Dordrecht, 1985, p. 75.
[24] A.C. Lasaga, J. Geophys. Res. 89 (1984) 4009.
[25] A.C. Lasaga, in: A.F. White, S.L. Brantley (Eds.), Rev. Miner. 31 (1995) 23.
[26] R.A. Berner, E.L. Sjoberg, M.A. Vebel, M.D. Krom, Science 207 (1980) 1205.
[27] R. Petrovic, Geochim. Cosmochim. Acta 40 (1976) 1509.
[28] G.R. Holdren Jr., R.A. Berner, Geochim. Cosmochim. Acta 43 (1979) 1161.

[29] W.H. Casey, G. Sposito, Geochim. Cosmochim. Acta 56 (1992) 3825.
[30] G. Furrer, W. Stumm, Geochim. Cosmochim. Acta 50 (1986) 1847.
[31] H.C. Hegelson, W.M. Murphy, P. Aagaard, Geochim. Cosmochim. Acta 78 (1984) 2405.
[32] A.E. Blum, A.C. Lasaga, Nature 331 (1988) 431.
[33] N. Dacheux, A.C. Thomas, B. Chassigneux, E. Pichot, V. Brandel, M. Genet, Mater. Res. Soc. Proc. 556 (1999) 85.
[34] N. Dacheux, A.C. Thomas, B. Chassigneux, V. Brandel, M. Genet, in: G.T. Chandler, X. Feng (Eds.), Environmental and Waste Management Technologies in the Ceramic and Nuclear Industries V, vol. 107, 2000, p. 333.
[35] A.E. Blum, A.C. Lasaga, Geochim. Cosmochim. Acta 55 (1991) 2193.
[36] R Swalin (Ed.), Thermodynamics of Solids, Wiley, New York, 1972, p. 387.
[37] N.M. Rose, Geochim. Cosmochim. Acta 55 (1991) 3273.
[38] S.A. Caroll, thesis, Northwestern University, Evanson, 1989.
[39] S.A. Caroll-Webb, J.V. Walther, Am. J. Sci. 290 (1998) 797.
[40] P.S. Schweda, in: E. Miles (Ed.), Water–Rock Interaction, Balkema, Rotterdam, 1989, p. 609.
[41] K.B. Helean, W. Lutze, R.C. Ewing, in: J.C. Marra, G.T. Chandler (Eds.), Environmental Issues and Waste Management Technologies in the Ceramics and Nuclear Industries IV, vol. 93, 1999, p. 297.
[42] A.E. Ringwood, S.E. Kesson, K.D. Reeve, D.M. Levins, E.J. Ramm, in: W. Lutze, R.C. Ewing (Eds.), Radioactive Waste Forms for the Future, North-Holland, Amsterdam, 1988, p. 233.
[43] S.T. Tso, J.A. Pask, J. Am. Ceram. Soc. 65 (1982) 360.
[44] A.C. Thomas, N. Dacheux, J. Aupiais, V. Brandel, M. Genet, to be published.
[45] J. Schott, R.A. Berner, E.L. Sjoberg, Geochim. Cosmochim. Acta (1981) 2123.
[46] International Centre for Diffraction Data, PDF database, Newton Square, PA.
[47] V. Brandel, N. Dacheux, M. Genet, to be published.
[48] N. Dacheux, V. Brandel, M. Genet, New J. Chem. 19 (1995) 15.
[49] N. Dacheux, V. Brandel, M. Genet, New J. Chem. 19 (1995) 1029.
[50] N. Dacheux, V. Brandel, M. Genet, K. Bak, C. Berthier, New J. Chem. 20 (1996) 301.
[51] D.E. Corbridge, in: M. Grayson (Ed.), Topics in Phosphorus Chemistry, Wiley, NewYork, 1966, p. 275.
[52] A.C. Chapman, L.E. Thirlwell, Spectrochim. Acta 20 (1964) 937.